Complex Systems

INTERMODULAR DESCRIPTION SHEET

TITLE	Complex Systems
PROJECT TEAM	Project Leader: Dr. Paul Isihara Fall ’23 Math 385 Topics in Applied Math Student Contributors: Taylor Chiles, Jadon Hsu, Aidan Kingsbury, Catherine Lamberson, Avery McKeaney, Jocelyn Rosa, and Harrison Stanton Department of Mathematics Wheaton College Wheaton, IL 60187
MATHEMATICAL FIELD	Complex System Science
APPLICATION FIELD	Urban Data Analysis, Human Disaster Migration
TARGET AUDIENCE	Students with a mathematical background interested in complexity applied to societal applications.
ABSTRACT	This Module introduces concepts from complex system science, their root in statistical physics, and their application to society. Concepts are illustrated using knowledge gained from an in-progress Math Serve supporting the relaunch of education and restoration of IDPs in Tigray, Ethiopia after a horrific two-year civil war.
PREREQUISITES	Differential Equations and Probability & Statistics

Contents

1. Introduction

1.1 Setting the Scene

A brutal two year civil war (Nov 2020-Nov 2022) crippled the entire infrastructure of the Tigray region of northern Ethiopia. All 6-7 million people in the region experienced trauma due to a large number of civilian deaths and victims of rape as a weapon of war, as well as a 2-year blockade of internet, cell phone communication, banking, and humanitarian aid. Today, there are food shortages everywhere, and hundreds of death by starvation have occurred during the writing of this Module. Poverty abounded everywhere during the war and continues to be a major problem with many women forced into prostitution for survival. Almost all medical services were incapacitated and doctors were among those left begging on the streets for food. In the education sector, over 2,000 schools were closed during the war. Without outside intervention, over two million children faced their third year out of school. To compound this already overwhelming scenario, one year after the Pretoria peace agreement was signed, fighting continued in the western part of Tigray, leaving 1 million internally displaced people (IDP) living in over 600 IDP camps scattered across the rest of the region (**Figure 1**). Maintaining a minimum holistic standard of living for one million IDP (food, water, sanitation, health, education, safety,...) is a complex problem. Is this a problem for the Tigray regional government to implement a well-orchestrated and funded policy across the region? (With all the other problems it faces, how high a priority can the regional government give to the IDP's?) Or, is this a problem requiring intervention by individuals, NGOs, and local district governments (woredas) who might make a difference for selected groups of IDP's?

Let's narrow our focus to the following scenario which considers just one aspect of the complex IDP problem. A small NGO involved in disaster relief has experience in supporting education within IDP camps. Data made available by the U.N.'s International Office for Migration (IOM) in August 2023 (https://data.humdata.org/dataset/ethiopia-displacement-northern-region-tigray-idps-site-assessment-iom-dtm?) includes information whether or not IDP camps have education needs in the following areas:

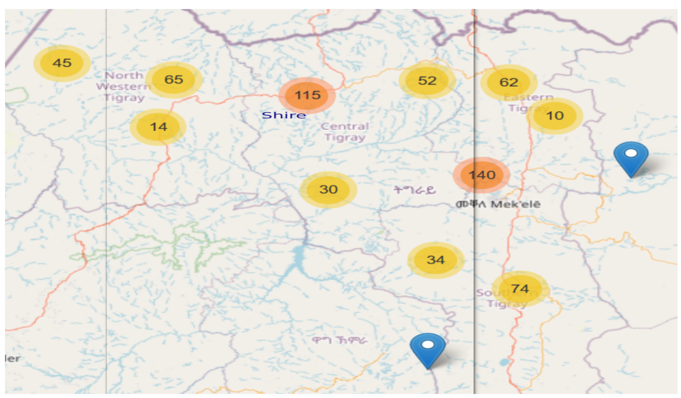

Figure 1. Map showing locations of 600+ IDP camps in Tigray. There were 1 million IDP living in camps at the time of writing of this Module. Map data: UN/IOM and Open Street Map

- pre-primary;
- secondary;
- resources;
- quality/satisfaction;
- girl attendance;
- boy attendance; and
- teachers.

To maximize effective impact in an efficient way, it would make sense for the NGO to base its efforts either in the regional capital (Mekelle) or the second largest city (Shire) since they have roughly half of all the IDP camps and half of the one million IDPs. Moreover, these cities have direct flights to and from Addis Ababa which is important for safety considerations. A specific question we pose here and re-visit at the end of this Module is: "which city has the greater need for the NGO's intervention due to a higher degree of educational disorder in its IDP camps?"

1.2 Complex System Science

This Module offers a brief introduction to complex system science. Complexity is an intuitive concept which arises across disciplines, including urban issues such as the problem of an influx of large numbers of displaced people. The science of complex systems seeks to develop a rigorous methodology for analyzing overall system behavior based on interactions involving a large number of constituent parts or agents. Analytical methods, including those arising from statistical physics, utilize a wide range of undergraduate level mathematics such as calculus, linear algebra, differential equations, and probability and statistics. Our goal is to show how a few important concepts found in these quantitative methods (for example, equilibrium, phase transition, and entropy) support basic notions of complex systems, and how they offer a perspective on practical questions in complex human society.

.

From a humanitarian standpoint, two goals of complex system science include:

- prevent dangerous misunderstanding and unjust practices associated with an erroneous view of complex social/environmental systems; and
- provide insights which can help facilitate enduring solutions to complex societal problems.

A classic example of a dangerous misunderstanding of a complex situation in Chicago is the urban redlining maps from the 1920's which classified neighborhoods with high density of African Americans as 'hazardous' and deemed mortgages not insurable by the F.H.A.. Redlining permanently crippled Black home ownership (see **Figure 2**, left panel). As for a recent example of a helpful insight into the same urban area, Robert Sampson [2012] introduced a concept called *collective efficacy* (cooperation between community members) suggesting that violent crime reduction might be facilitated by a coherent community-based approach (**Figure 2** right panel).

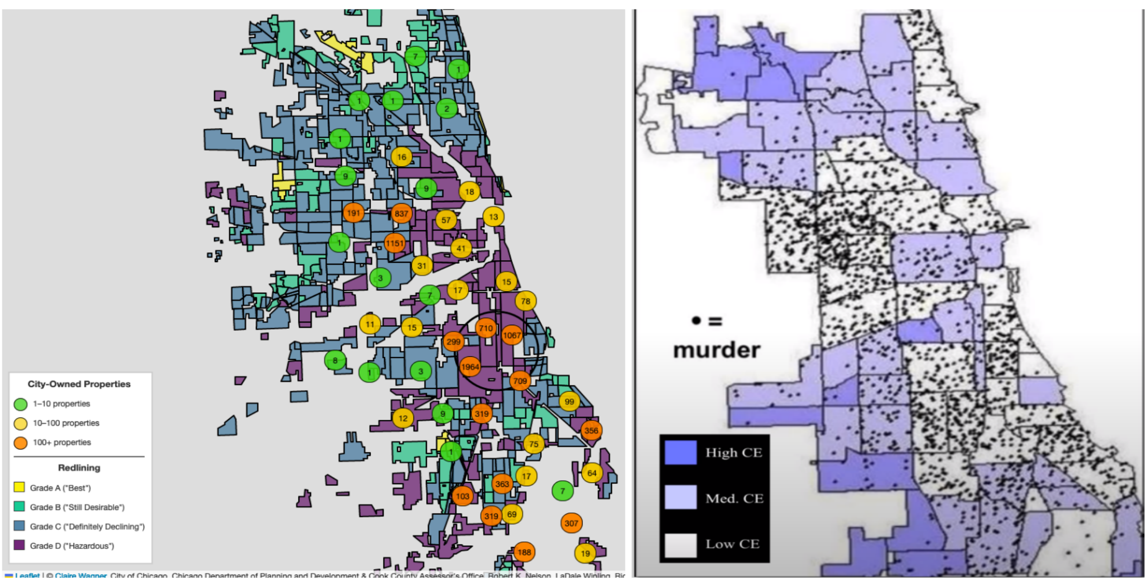

Figure 2. (Left) Home Owners' Loan Corporation neighborhood classifications and present day city owned empty lots. The circled area with a high concentration of empty lots was labeled 'Hazardous'. Map Credit: Claire Wagner (Right) Collective efficacy (CE) levels and homicides. Map credit: Robert Sampson https://www.youtube.com/watch?v=gEXSOUqwztA (Used with permission of the author.)

This Module is organized into three sections:

- Fundamental Concepts (**Section 2**);
- Mathematical Formalism from Statistical Physics (**Section 3**); and
- Societal Applications (**Section 4**).

The Exercises are an integral part of this Module, and should at least be read if not attempted in earnest (solutions to the Exercises are included at the end of the Module). Python Jupyter Notebooks (JNBs) are also an important part of this Module and available to the reader at https://drive.google.com/drive/folders/1zqQB-hEPocxOVOjiI0Q32XDKVJoq6PI3?usp=sharing, as well as the Journal's supplementary materials.

2. Fundamental Concepts

In this section we describe qualitatively several concepts which are basic when studying complex systems.

2.1 Homogeneity of Constituent Parts

One basic difference between pure physical science and a study of human society is an assumption about the degree of homogeneity of the constituent parts of a system. Statistical physics methodology applied to an ensemble of identical gas molecules is simpler than application to a society comprised of unique individuals with different values, decision-making, propensity to do good or evil etc.. Systems where a homogeneity assumption of the constituent units is reasonable (eg. large flock of birds in synchronized flight) are more amenable to mathematical approaches.

Exercise

2.1 Referring to Figure 3 explain how the degree of homogeneity of the constituent jig saw pieces relates to the overall complexity of the jigsw puzzle.

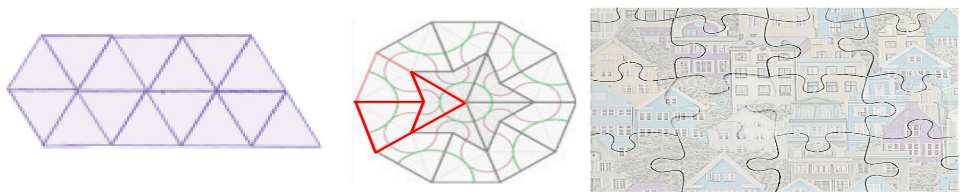

Figure 3. Left: 1 piece jigsaw puzzle (crystal) Center: 2 piece 'kite and dart' jigsaw puzzle (quasicrystal) Right: Random piece jigsaw puzzle of an urban neighborhood.

2.2 System Classification

In standard undergraduate math courses, we are introduced to basic ways to distinguish equations or models such as linear vs. non-linear, discrete vs. continuous, and random vs. deterministic. These categories continue to be important in complex system science, with additional types of classification helpful in understanding system behavior.

Open, Closed, and Isolated Systems

Systems can be classified according to whether they exchange energy or mass with the environment:

- ISOLATED: system exchanges neither mass nor energy with its environment;
- CLOSED: system exchanges energy but not mass with its environment; or
- OPEN: system exchanges both mass and energy with its environment.

Note that in studying complex human society, energy exchange may be broadly defined (for example, a remote exchange of ideas or financial credit.)

Random, Correlated, and Coherent Systems

Another important type of system classification is based on how the individual components are related to each other [Siegenfeld and Bar-Yam 2020]:

- RANDOM: Each component behaves independently of the others;
- COHERENT: Each component behaves in the same way; or
- CORRELATED: Systems which are in between random and coherent systems.

For example, the direction of passengers seated on a 14 hour airplane flight during takeoff is coherent, the length of time they sleep during flight is random, and their choice of in-flight entertainment is correlated.

Entropy is a measure of disorder of a system. Random systems have large entropy, and perfectly coherent systems zero entropy. Complex systems may undergo phase transitions from coherent states with zero entropy to correlated/random states with positive entropy.

Emergent Global Behavior

Models can help explain how recognizable macroscopic or global states emerge from microscopic or local interactions. For example, synchronized movement (coherence) of a flock of birds can be modelled as emergent macroscopic system behavior based on a few simple local rules [Tranquillo 2019] (https://www.youtube.com/watch?v=nbbd5uby0sY)

- SEPARATION: Birds keep a minimum distance from other birds;
- ALIGNMENT: Birds move towards the average direction of the neighbors they see around them; and
- COHESION: Birds move towards the average center of mass of the birds around them.

Exercises

2.2.1 During the civil war, Tigray was suppressed into a closed system. Shortly after the war ended in November 2022, UNICEF reported over 2,000 schools were closed (https://www.overleaf.com/project/64cea7ed189af9e4b7c1ba38). Elementary school students' walk to school increased from 1 to 4 miles, and student to classroom ratios were over 400:1. Without blackboards, a teacher resorted to use of a large stone in working with students (**Figure 4**).

Figure 4. A teacher used a rock in lieu of a blackboard as a result of the ransacking/blockade of Tigray during the civil war.

How would the rebuilding of education be different within an isolated, closed, or open educational system?

2.2.2 How might coherence (or lack thereof) of IDP camps impact the complexity of a response?

2.2.3 Show that a clearly visible pattern emerges if we apply Stephen Wolfram's Rule 90 to a single black square on a large graph paper (https://mathworld.wolfram.com/SierpinskiSieve.html). The rule explains the coloring of squares on the row below the current row.

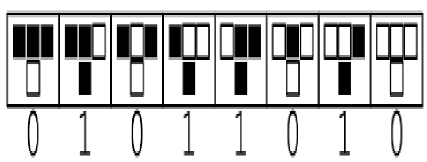

Figure 5. Wolfram Rule 90.

2.3 Linearization

Linear systems are foundational and a starting point for the study of dynamical systems. Nonlinear systems are needed to model complexity and have been important in the study of dynamical systems for the past 50 years. In general, non-linear systems do not have exact solution methods. Non-linear systems may be approximated by linear systems near equilibrium points.

Consider a non-linear system

$$\begin{aligned} x' &= f(x, y) \\ y' &= g(x, y). \end{aligned}$$

An equilibrium point (x^*, y^*) for the non-linear system satisfies

$$\begin{aligned} f(x^*, y^*) &= 0 \\ g(x^*, y^*) &= 0. \end{aligned}$$

The Jacobian matrix (all partials are evaluated at the equilibrium point) is

$$J = \begin{pmatrix} \frac{\partial f}{\partial x} & \frac{\partial f}{\partial y} \\ \frac{\partial g}{\partial x} & \frac{\partial g}{\partial y} \end{pmatrix}.$$

If the real part of the eigenvalues of the Jacobian matrix are non-zero, then the behavior of the non-linear system at the equilibrium point (x^*, y^*) is given qualitatively by the behavior of the equilibrium point at (0,0) of the linear system

$$\begin{pmatrix} v' \\ w' \end{pmatrix} = J \begin{pmatrix} v \\ w \end{pmatrix}.$$

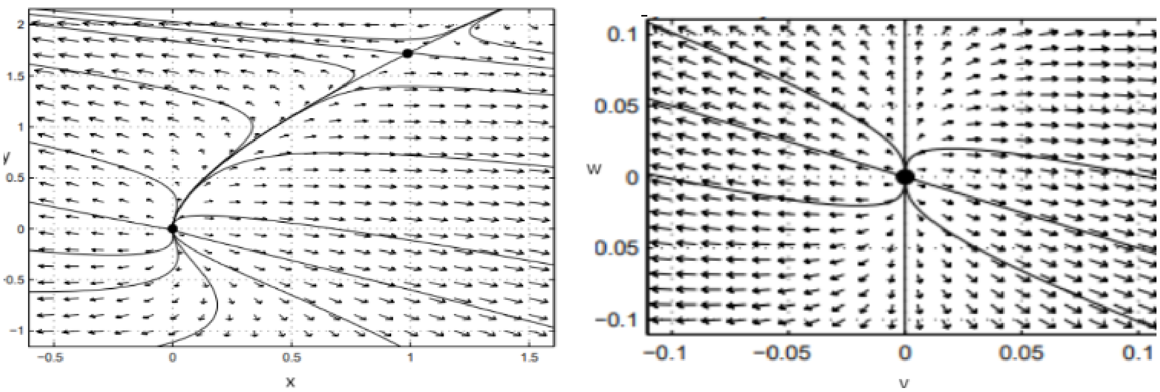

Figure 6. (Left) Nonlinear solutions (Right) Linearization at the equilibrium point (0,0)

Let A be the Jacobian matrix for a linearized 2-D non-linear system at an equilibrium point $P = (x^*, y^*)$. **Figure 7** summarizes the qualitative behavior of the nonlinear system near P (**Exercise 2.3.1**).

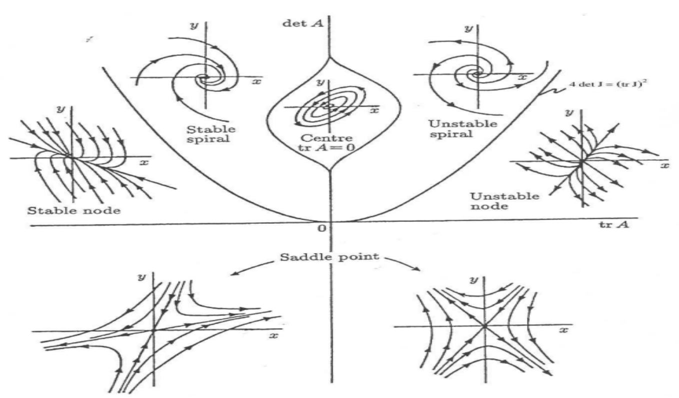

Figure 7. Classification of equilibria for linearized 2-D systems. Figure Credit: Appendix A of J.D. Murray's [2002] *Mathematical Biology*. (Used with permission of the author.)

Logistic Growth

Moving away from an equilibrium point, the need to transition from an approximating linear behavior to non-linear behavior is illustrated using COVID-19 data shown in **Figure 8**. Mathematically, let k and M be positive constants, and consider the logistic growth equation

$$\frac{dz}{dt} = kz(1 - \frac{z}{M}),$$

with $z(0) = z_0$ positive and close to 0. Note that when z/M is small, the linear exponential growth model $\frac{dz}{dt} = kz$ is a good approximation for the nonlinear logistic model. Over time, as $z \to M$, the non-linearity which arises from multiplication of kz by $(1 - \frac{z}{m})$ is needed to cap the long range growth by reducing the value of $\frac{dz}{dt} = kz(1 - \frac{z}{m})$ to zero.

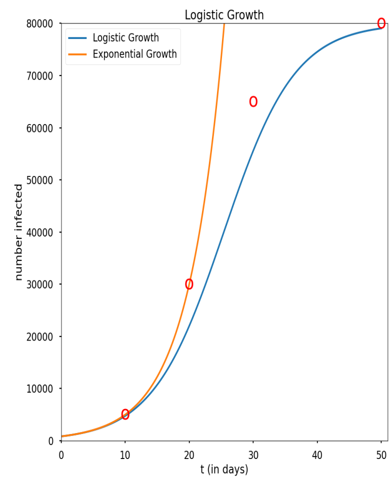

Figure 8. COVID-19 data plotted as circular points together with exponential and logistic growth curves.

For simplicity, set $k = 2$, $M = 2$ so that $\frac{dz}{dt} = g(z) = 2z - z^2$. The stability of the equilibrium when $z = 2$ can be inferred from the local minimum point of a potential function $V(z) = -z^2 + \frac{1}{3}z^3$ (**Figure 9**) which satisfies $V'(z) = -g(z)$. When $z > 2$, $V'(z) > 0 \Rightarrow \frac{dz}{dt} < 0$ (so z decreases towards the equilbrium value); and when $z < 2$, $V'(Z) < 0 \Rightarrow \frac{dz}{dt} > 0$ (so z increases towards the equilibrium value. The idea that optimization of an auxiliary function (in this case the potential $V(z)$) can be used to analyze system behavior will be important in **Section 3**.

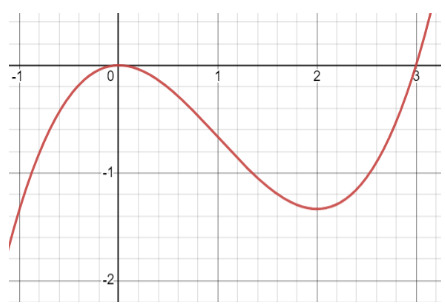

Figure 9. The minimum point on the potential function $V(z) = -z^2 + \frac{1}{3}z^3$ corresponds to the stable equilibrium $z = 2$.

Exercises

2.3.1 Let A be the Jacobian matrix for a linearized 2-D non-linear system at an equilibrium point $P = (x^*, y^*)$. Use **Figure 7** to explain how eigenvalues of A can be used to find the following qualitative behavior of the nonlinear system near P.

2.3.2 Use linearization to describe the behavior of the following system near its equilibrium at (0,0):

$$\begin{aligned}\frac{dx}{dt} &= 3x - y^2\\ \frac{dy}{dt} &= sin(y) - x.\end{aligned}$$

2.4 Bifurcations

It is often the case that the behavior of a physical system is dependent on a parameter value such as temperature. In some cases, there is a critical parameter value at which the macroscopic state of a system undergoes a fundamental change in behavior (for example, transition of water from liquid to solid state).

Consider a natural environment with two types of animals: a single predator (eg. foxes) and a single prey (eg. rabbits). There are different possibilities for the equilibrium states of the predator density F^* and prey density C^*:

- the predator population dies off ($F^* = 0$) for lack of food and there is a stable number of prey ($C_* > 0$) that remains;
- there is a stable number of both predators and prey ($F^* > 0, C^* > 0$); or
- the number of predators and prey cycle periodically (see **Figure 10**).

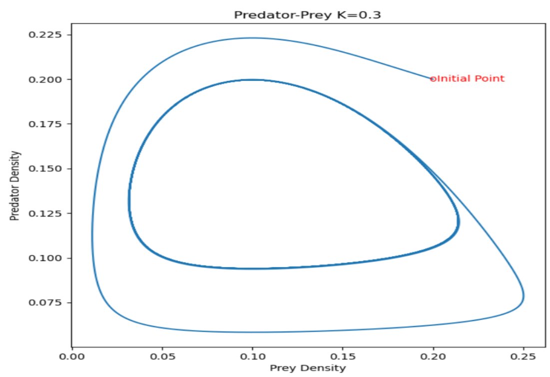

Figure 10. A predator-prey model which exhibits a stable limit cycle seen in the middle region of the diagram. The number of predator and prey both fluctuate periodically.

For this system, the carrying capacity K of the predator population is a bifurcation parameter (See **Figure 11** and **Exercise 2.3.1**):

- When $K > 0$ is small, a stable steady state occurs at $(F, C) = (0, C_*)$ with $C_* > 0$.
- For higher values of K, the equilibrium $(0, C_*)$ loses its stability and there arises a new stable equilbrium (sink) (F^*, C^*) with $F^* > 0$ and $C^* > 0$.
- For even higher values of K, this equilibrium (F^*, C^*) becomes a stable spiral sink.
- For still higher values of K, the equilibrium (F^*, C^*) loses its stability and a stable limit cycle (closed curve) solution appears.

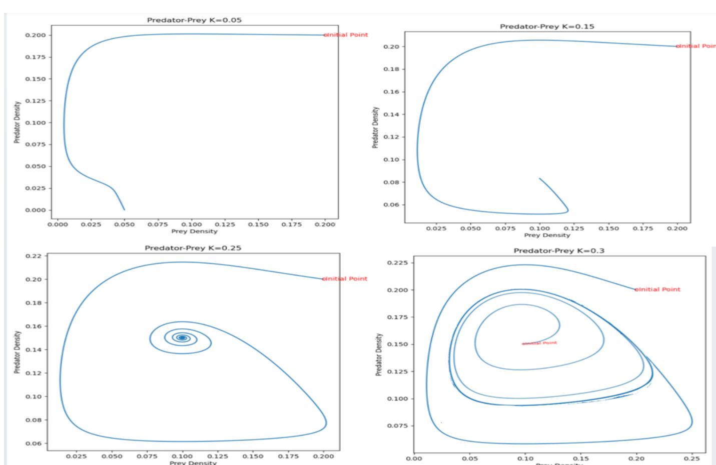

Figure 11. Bifurcation in the Predator-Prey Equations

Exercises

2.4.1 Consider the Rosenzweig-MacArthur (RM) predator-prey model [Martin and de Roos 2023]

$$\begin{aligned}\frac{dF}{dt} &= rF(1-\frac{F}{K}) - \frac{aF}{1+ahF}C \\ \frac{dC}{dt} &= \epsilon\frac{aF}{1+afF}C - \mu C\end{aligned}$$

where

- $F =$ prey density (eg rabbits)
- $C =$ predator density (eg foxes)
- $\frac{dF}{dt}$ = dynamic change of prey
- $\frac{dC}{dt}$ = dynamic change of predator
- r = prey natural growth rate
- K = prey carrying capacity
- a = attack rate
- h = handling rate (predator needs h time units to consume prey)
- e = prey offspring proportionality constant
- μ = predator death rate.

Use a JNB to confirm that

- When $K > 0$ is small, a stable steady state occurs at $(F, C) = (0, C_*)$ with $C_* > 0$.
- For higher values of K, the equilibrium $(0, C_*)$ loses its stability and there is a steady equilibrium (sink) (F^*, C^*) with $F^* > 0, C^* > 0$.
- For even higher values of K, the equilibrium (F^*, C^*) is a spiral sink.
- For still higher values of K, the equilibrium (F^*, C^*) loses its stability and a stable limit cycle (closed curve) solution appears.

2.4.2 The RM model exhibits what is called a Hopf bifurcation, as described in the schematic below:

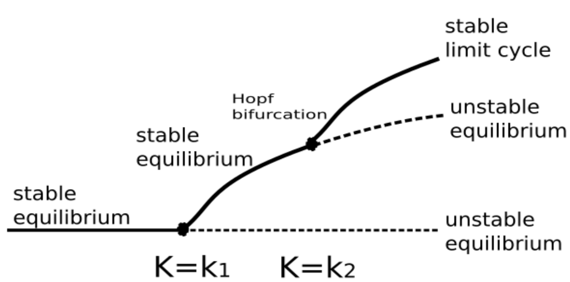

Figure 12. Problem 2.4.2.

Explain how the Hopf bifurcation diagram corresponds to your solution to **Exercise 2.4.1**.

2.4.3 One dimensional maps can also undergo bifurcations. For example, consider the 1-D map $x_{n+1} = rx_n(1 - x_n)$.

a) Find the period one point (fixed point) for this map when $r < 2$.

b) This map undergoes a period doubling bifurcation as shown in **Figure 13**. What type of universality is suggested by this sequence of bifurcations?

Period	Bifurcation parameter (r)	Ratio $\left(\frac{r_{n-1}-r_{n-2}}{r_n-r_{n-1}}\right)$
2	3.0	–
4	3.449	–
8	3.544	4.7514
16	3.564	4.6562
32	3.658	4.6683
64	3.569	4.6686
128	3.5696	4.6692
256	3.5699	4.6694

Figure 13. Exercise 2.4.3 b)

2.5 Normal vs. Power-Law Random Behavior

A system which evolves over time is deterministic if its future states are modelled by a deterministic function of time. In contrast, future states may depend on a random process. One-dimensional random walks are among the simplest type of non-deterministic systems. Let x_t denote the position at discrete times $t = 0, 1, 2, ...$ of an object moving at random on a one-dimensional integer lattice. Consider a random walk with $x_0 = 0$ and

$$x_{t+1} = x_t + e_t$$

where $e_t = \pm 1$ with equal probability. The random variables e_t and $e_{t'}$ $(t \neq t')$ are assumed to be independent and identically distributed (IID).

A single random walk is impossible to predict, and any observed trend in a specific random walk is not in general a common feature of all random walks. Yet, a large number of random walks will have a predictable expected position $< x_t >= 0$ and variance $< x_t^2 >= t$ (**Figure 14**) since

- $< x_{t+1} >=< x_t > + < e_t >=< x_t >=< x_0 >= 0$ for all t; and
- $< x_{t+1}^2 >=< x_t^2 > +2 < x_t >< \epsilon_t > +1 =< x_t^2 > +1 \Rightarrow < x_t^2 >=< x_0^2 > +t = t$.

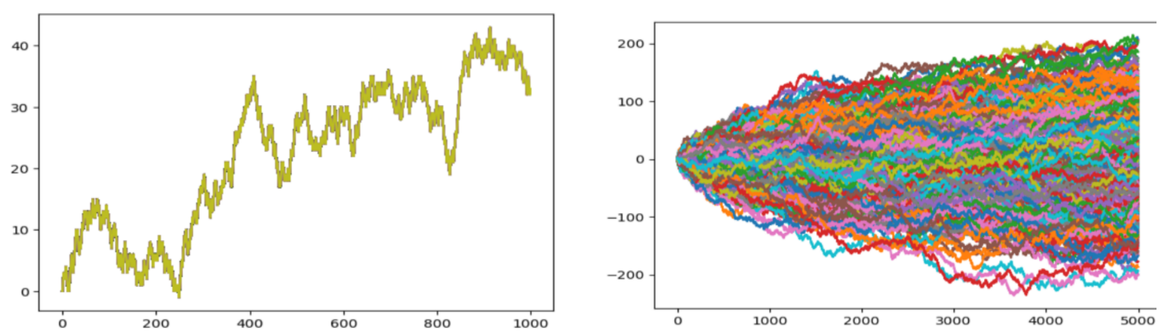

Figure 14. (Left) A single random walk is unpredictable. (Right) A large number of random walks have predictable mean $< x_t >= 0$ and variance $< x_t^2 >= t$.

We can also create a random walk using variable step sizes by random draws from a continuous probability distribution. **Figure 15** shows the difference between random walks which are normal vs. Cauchy (power-law) distributed. The former gives rise to two-dimensional Brownian motion where both the x and y step sizes are normally distributed. Very large steps sizes have negligible probability of occurrence and are not observed. On the other hand, large step sizes ('long-flights') are observed in power-law (heavy-tail) distributed random walks. These may correspond to catastrophic events (eg. a stock market crash). Complex systems are often characterized by power-law behavior [Fieguth 2021].

Exercise

2.5 Use a JNB to re-create the graphs in **Figure 15**.

3. Mathematical Concepts from Equilibrium Statistical Physics

Many important concepts in the study of complex systems trace back to the highly mathematical field of statistical physics. This section touches on just a few of these concepts for equilibrium systems following [Bertin 2022]:

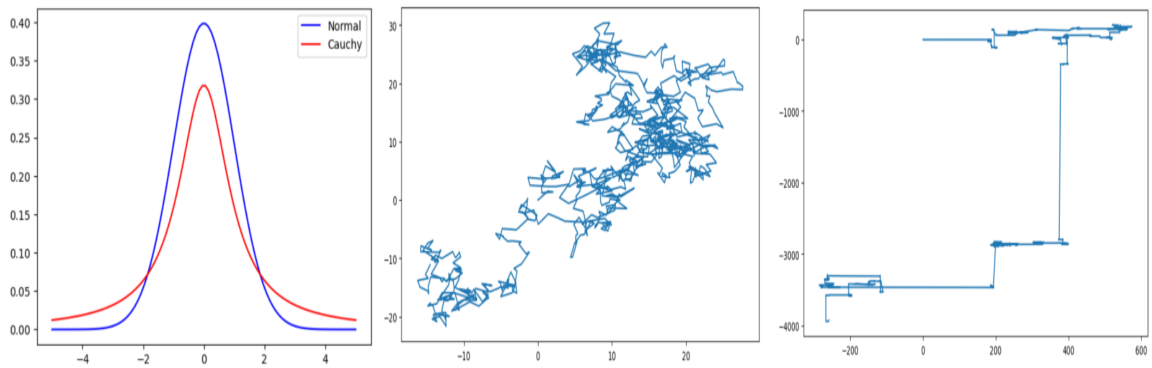

Figure 15. (Left) Normal and Cauchy (power-law) distributions. (Center) Brownian motion with moves normally distributed. (Right) Heavy tail of a Cauchy distribution gives rise to 'long-flights' in the random walk.

- the Hamiltonian (total energy) of a system in equilibrium (**Section 3.1**);
- discrete Ising spin models and entropy for systems with a specified energy (**Section 3.2**); and
- maximum likelihood states and phase transitions involving a change in a system parameter such as temperature T (**Section 3.3**).

The section concludes with a simplified Schelling model (**Section 3.4**) as an example how a statistical physics approach can model segregation in society.

3.1 The Hamiltonian

For systems in equilibrium, the Hamiltonian can illustrate important concepts such as conservation of energy and time reversibility.

Spring Mass Problem

An idealized spring-mass model considers a mass m attached to a spring which exerts the total force F on the mass moving in 1 dimension:

$$F = -kx. \tag{1}$$

Here $k > 0$ is a spring constant, and x is the distance the spring is stretched ($x > 0$) or compressed ($x < 0$) from its rest position at $x = 0$.

From Newton's 2nd Law, we know that $F = ma$, which leads to the ODE

$$mx''(t) = -kx. \tag{2}$$

The general solution is $x(t) = A\cos(\omega t + \phi)$, where $\omega = \sqrt{\frac{k}{m}}$. This indicates that the motion is periodic in the absence of any frictional or damping forces.

Total Energy (Hamiltonian)

In this idealized model, the total energy of the spring-mass system is conserved, so the solution indicates that a periodic oscillation will continue for all t. Hamiltonian dynamics focuses on the system's total energy, denoted H (for Hamiltonian) or E (for energy). The total energy is the sum of kinetic energy ($\frac{1}{2}mv^2$) and potential energy U. Note that momentum $p = p(t)$ is defined as $p(t) = mv(t) = mx'(t)$ so the kinetic energy in terms of p is equal to $\frac{p^2}{2m}$. The potential function U is related to the conservative force F according to

$$U'(x) = -F(x). \tag{3}$$

It follows that the potential energy is $U(x) = \frac{1}{2}kx^2$.

Summing the kinetic and potential energy, gives the Hamiltonian

$$H(x,p) = \frac{p^2}{2m} + \frac{1}{2}kx^2. \tag{4}$$

Properties of the 1-D Hamiltonian Dynamics

Suppose our starting point for analyzing 1-D dynamics is to give the total energy in terms of the Hamiltonian $H(x,p) = \frac{p^2}{2m} + \frac{1}{2}kx^2$ obtained in **(4)**. We could then show that the following hold:

- (Dynamical Equations) The state vector consisting of position and momentum $< x(t), p(t) >$, satisfies (**Exercise 3.1.1**)

$$\begin{aligned} \frac{dx}{dt} &= \frac{\partial H}{\partial p} \\ \frac{dp}{dt} &= -\frac{\partial H}{\partial x}. \end{aligned}$$

- (Energy Conservation) Conservation of energy can be proven (**Exercise 3.1.2**) by showing that if $E = H(x,p)$, then

$$\frac{dE}{dt} = 0.$$

  Note that as a consequence, if we let

$$X = \sqrt{\frac{k}{2}}x, \qquad Y = \frac{p}{\sqrt{2m}}$$

  then in (X,Y) *phase space*, the particle's trajectory is along a circle

$$X^2 + Y^2 = E.$$

- (Time Reversibility) Time reversibility means that the dynamical equations for the time interval ($0 \le t \le t_0$) are invariant under the transformations

$$\begin{aligned} t &\rightarrow t^* = t_0 - t \\ x = x(t) &\rightarrow x^* = x(t^*) \\ v = \frac{dx(t)}{dt} &\rightarrow v^* = \frac{dx^*}{dt^*} = -\frac{dx^*}{dt} = -\frac{dx(t^*)}{dt} = -v(t^*) \\ p = p(t) &\rightarrow p^* = mv^* = -mv(t^*) \end{aligned}$$

  The Hamiltonian $H = H(x^*, p^*) = \frac{(p^*)^2}{2m} + \frac{1}{2}k(x^*)^2$ for time reversal specifies the dynamical equations (**Exercise 3.1.3**)

$$\begin{aligned} \frac{dx^*}{dt^*} &= \frac{\partial H}{\partial p^*} \\ \frac{dp^*}{dt^*} &= -\frac{\partial H}{\partial x^*}. \end{aligned}$$

  That is, the time-reversed state vector $< x^*, p^* >$ is also a feasible dynamical trajectory.

The Hamiltonian for a single particle in 1-D can be generalized to describe the dynamics of N particles in higher dimensional space. Conservation of energy and time reversibility continue to hold. Moreover, we state the

FUNDAMENTAL POSTULATE OF EQUILIBRIUM STATISTICAL PHYSICS:

In equilibrium, the total energy E is conserved, and all configurations with energy E are uniformly probable.

Exercises

These problems are based on the idealized 1D spring-model whose dynamics are given by the ODE

$$mx''(t) = -kx \tag{5}$$

with general solution $x(t) = A\cos(\omega t + \phi)$, where $\omega = \sqrt{\frac{k}{m}}$.

3.1.1 Show that

$$\begin{aligned}\frac{dx}{dt} &= \frac{\partial H}{\partial p}\\ \frac{dp}{dt} &= -\frac{\partial H}{\partial x}\end{aligned}$$

where H is the Hamiltonian given by $H(x,p) = \frac{p^2}{2m} + \frac{1}{2}kx^2$.

3.1.2 Use a chain rule for 2 variables to show that if $E = H(x,p)$, then $\frac{dE}{dt} = 0$.

3.1.3 Show that under the the transformations

$$\begin{aligned} t &\rightarrow t^* = t_0 - t\\ x = x(t) &\rightarrow x^* = x(t^*)\\ v = \frac{dx(t)}{dt} &\rightarrow v^* = \frac{dx^*}{dt^*} = -\frac{dx^*}{dt} = -\frac{dx(t^*)}{dt} = -v(t^*)\\ p = p(t) &\rightarrow p^* = mv^* = -mv(t^*)\end{aligned}$$

the Hamiltonian $H = H(x^*,p^*) = \frac{(p^*)^2}{2m} + \frac{1}{2}k(x^*)^2$ specifies the dynamical equations

$$\begin{aligned}\frac{dx^*}{dt^*} &= \frac{\partial H}{\partial p^*}\\ \frac{dp^*}{dt^*} &= -\frac{\partial H}{\partial x^*}.\end{aligned}$$

That is, the time-reversed state vector $< x^*, p^* >$ is also a possible dynamical trajectory.

3.2 Ising Spin Models and Entropy

Ensembles of a finite number of particles can be classified according to whether they exchange energy or mass with their environment:

- *microcanonical ensemble* An isolated system $\mathcal{S}$ which exchanges neither energy nor mass with its environment $\mathcal{R}$.
- *canonical ensemble* A system $\mathcal{S}$ which exchanges energy with its environment $\mathcal{R}$. The total system $\mathcal{S} \cup \mathcal{R}$ is assumed to be isolated.
- *grand-canonical ensemble* A system $\mathcal{S}$ which exchanges both mass and energy with its environment $\mathcal{R}$. The total system $\mathcal{S} \cup \mathcal{R}$ is assumed to be isolated.

The Ising model is a simple discrete model which can be used to study energy and mass exchange of a system with its environment, as well as phase transitions. For our discrete model, we restrict particle positions to a lattice of evenly spaced points in dimension D=1 or 2. For example, the points on a number line representing the integers $\mathbb{Z}$ form a 1-D lattice. Similarly, the points with integer coordinates $\{(m,n) \mid m,n \in \mathbb{Z}\}$ forms a 2-D lattice. A system of N particles may be confined to a certain portion of the lattice by a boundary, and exchange energy or mass with its environment (lattice points outside the boundary which may be occupied by other particles). Time is incremented in discrete time steps $t_0, t_1, t_2, ...$

A *spin system* assigns a value of +1 or -1 to each particle. The Hamiltonian or total energy E of the system is computed using the spin values. In the basic Ising model for an N particle system,

$$E = -J\sum_{i,j} s_i s_j - h\sum_{i=1}^{N} s_i \tag{6}$$

where

- the values of i,j in the first sum run over a specified set of lattice points such as "nearest neighbors" . For example, in dimension $D = 1$, a particle has 2 nearest neighbors, and in $D = 2$, there are 4 nearest neighbors.

- $J \geq 0$ is called the *spin coupling constant*. ($J = 0$ if the spins are independent of each other, i.e. totally decoupled).
- $h \geq 0$ is the external magnetic field constant and the magnetization M is equal to

$$M = \sum_{i=1}^{N} s_i \qquad (s_i = \pm 1).$$

- a state or configuration C is specified by a complete list of spin values $(s_1, ..., s_N)$.
- $\Omega(E)$ is the number of configurations with energy E.
- if E is the energy of the system in equilibrium, all spin configurations with energy E have equal positive probability of occurrence and all other configurations have zero probability of occurrence.

Isolated Paramagnetic Spin Model

For the case of independent spins, we set $J = 0$, and the energy E simplifies to

$$E = -h \sum_{i=1}^{N} s_i = -hM, \quad (s_i = \pm 1),$$

where $M = \sum_{i=1}^{N} s_i$ is the magnetization.

Given the energy E, let N_+ be the number of particles with spin +1 and N_- be the number of particles with spin -1. Using algebra, we can show (**Exercise 3.2.1**) that

$$N_+ = \frac{1}{2}(N - \frac{E}{h})$$

and

$$N_- = \frac{1}{2}(N + \frac{E}{h}).$$

It follows that

$$\Omega(E) = \frac{N!}{N_+! N_-!}$$

The entropy $\mathbf{S}(E)$ is computed as

$$\mathbf{S}(E) = \ln \Omega(E).$$

Using Stirling's formula

$$\ln N! \approx N \ln N - N,$$

the entropy $\mathbf{S}$ of the parametric spin model of a system with energy E is (**Exercise 3.2.2**)

$$\mathbf{S}(E) \approx \ln \frac{N^N}{N_-^{N_-} N_+^{N_+}}.$$

Canonical Ensembles

We now consider a canonical equilibrium system $S_{tot} = \mathcal{S} \cup \mathcal{R}$ where system $\mathcal{S}$ exchanges energy with its environment $\mathcal{R}$. The total system $S_{tot} = \mathcal{S} \cup \mathcal{R}$ is considered to be a closed system.

- The total energy $E_{tot} = E_{\mathcal{S}} + E_{\mathcal{R}}$ is constant although energy can be exchanged between $\mathcal{S}$ and $\mathcal{R}$.
- A total system configuration (state) C_{tot} is written as $C_{tot} = (C_{\mathcal{S}}, C_{\mathcal{R}})$ where $C_{\mathcal{S}}$ is a configuration of $\mathcal{S}$ and $C_{\mathcal{R}}$ is a configuration of $\mathcal{R}$.
- $\Omega_{tot}(E_{\mathcal{S}} \mid E_{tot}) = \Omega_{\mathcal{S}}(E_{\mathcal{S}})\Omega_{\mathcal{R}}(E_{tot} - E_{\mathcal{S}}) = \Omega_{\mathcal{S}}(E_{\mathcal{S}})\Omega_{\mathcal{R}}(E_{\mathcal{R}})$. (Given the total energy E_{tot}, for a system energy $E_{\mathcal{S}}$, the admissible configurations of $\mathcal{S}$ and $\mathcal{R}$ are considered to be statistically independent.)

Under maximum likelihood, the most probable value $E^*_{\mathcal{S}}$ of $E_{\mathcal{S}}$ satisfies

$$\frac{\partial}{\partial E_{\mathcal{S}}} \mid_{E^*_{\mathcal{S}}} \ln \Omega_{tot}(E_{\mathcal{S}} \mid E_{tot}) = 0.$$

From this it follows that (**Exercise 3.2.3**)

$$\frac{\partial \ln \Omega_{\mathcal{S}}}{\partial E_{\mathcal{S}}} \mid_{E_{\mathcal{S}^*}} = \frac{\partial \ln \Omega_{\mathcal{R}}}{\partial E_{\mathcal{R}}} \mid_{E_{\mathcal{R}^*}}$$

where $E_{\mathcal{S}^*} + E_{\mathcal{R}^*} = E_{tot}$. The common value of the partial derivatives at the maximum likelihood energy is denoted β and called the "statistical temperature". For large systems, it can be shown that [Bertin 2021]

$$\beta = \frac{\partial \mathbf{S}_{tot}}{\partial E_{tot}}$$

where $\mathbf{S}_{tot} = \ln \Omega_{tot}$ is the entropy of the total system. A law of thermodynamics states that for physical systems $dE_{tot} = T d\mathbf{S}_{tot}$ where T is the usual thermodynamic temperature. Hence, $\beta = 1/T$.

Grand Canonical Ensembles

For a grand-canonical (GC) ensemble, the macroscopic system $\mathcal{S}$ exchanges both energy and particles with the environment $\mathcal{R}$. The modeling of GC ensembles is a natural extension of the modeling of canonical ensembles [Bertin 2021].

- Total energy: $E_{tot} = E_{\mathcal{S}} + E_{\mathcal{R}}$
- Total number of particles: $N_{tot} = N_{\mathcal{S}} + N_{\mathcal{R}}$
- Probability of Configuration $C_{\mathcal{S}}$:

$$\begin{aligned} P_{GC}(C_{\mathcal{S}}) &= K\Omega_{\mathcal{R}}(E_{tot} - E_{\mathcal{S}}(C_{\mathcal{S}}), N_{tot} - N_{\mathcal{S}}(C_{\mathcal{S}})) \\ &= K exp[\mathbf{S}_{\mathcal{R}}(E_{tot} - E_{\mathcal{S}}, N_{tot} - N_{\mathcal{S}}(C_{\mathcal{S}})] \end{aligned}$$

  where $K = 1/Z_{GC}$ is a normalization constant.

The linear approximation of $A = \mathbf{S}_{\mathcal{R}}(E_{tot} - E_{\mathcal{S}}, N_{tot} - N_{\mathcal{S}})$ is

$$A = \mathbf{S}_{\mathcal{R}}(E_{tot}, N_{tot}) - \beta E(C_{\mathcal{S}}) + \frac{\mu}{T} N_{\mathcal{S}}$$

where $\beta = 1/T$ is the statistical temperature and $\mu = -T \frac{\partial S_{\mathcal{R}}}{\partial N_{\mathcal{R}}}$ is called the chemical potential.

The grand-canonical partition function is defined as

$$Z_{GC} = \sum_{C_{\mathcal{S}}} exp[-\frac{1}{T} E(C_{\mathcal{S}}) + \frac{\mu}{T} N_{\mathcal{S}}(C_{\mathcal{S}})].$$

In terms of the partition function, the probability of configuration $C_{\mathcal{S}}$ (called the grand-canonical distribution) is

$$P_{GC}(C_{\mathcal{S}}) = \frac{1}{Z_{GC}} exp[-\frac{1}{T} E_{\mathcal{S}}(C_{\mathcal{S}}) + \frac{\mu}{T} N_{\mathcal{S}}(C_{\mathcal{S}})]$$

Exercises

3.2.1 Show that the following hold for the paramagnetic spin model with

$$E = -h \sum_{i=1}^{N} s_i, \qquad (s_i = \pm 1,)$$

$$N_+ = \frac{1}{2}(N - \frac{E}{h})$$

and

$$N_- = \frac{1}{2}(N + \frac{E}{h}).$$

3.2.2 Use Stirling's approximation to show that the entropy for the paramagnetic spin model of a system with energy E is given by

$$\mathbf{S}(E) \approx \ln \frac{N^N}{N_-^{N_-} N_+^{N_+}}.$$

3.2.3 Under maximum likelihood, the most probable value $E_{\mathcal{S}}^*$ of $E_{\mathcal{S}}$ satisfies

$$\frac{\partial}{\partial E_{\mathcal{S}}} |_{E_{\mathcal{S}}^*} \ln \Omega_{tot}(E_{\mathcal{S}} \mid E_{tot}) = 0.$$

Show that this implies

$$\frac{\partial \ln \Omega_{\mathcal{S}}}{\partial E_{\mathcal{S}}} |_{E_{\mathcal{S}^*}} = \frac{\partial \ln \Omega_{\mathcal{R}}}{\partial E_{\mathcal{R}}} |_{E_{\mathcal{S}^*}}$$

3.2.4 Explain the intuition behind the formula for the grand-canonical distribution:

$$P_{GC}(C_{\mathcal{S}}) = \frac{1}{Z_{GC}} exp[-\frac{1}{T} E_{\mathcal{S}}(C_{\mathcal{S}}) + \frac{\mu}{T} N_{\mathcal{S}}(C_{\mathcal{S}})].$$

3.2.5 In information theory, Shannon entropy is defined as

$$\mathbf{S} = -\sum_C P(C) \ln P(C).$$

Show that

a) For a microcanonical ensemble with energy $E_{\mathcal{S}}$, the Shannon entropy $\mathbf{S_{mic}} = -\sum_{C_{\mathcal{S}}} P(C_{\mathcal{S}}) \ln P(C_{\mathcal{S}})$ is given by

$$\mathbf{S_{mic}} = \ln \Omega(E).$$

b) For a canonical ensemble, recalling that $P_{\mathcal{S}}(C_{\mathcal{S}}) = \frac{1}{Z} e^{-E(C_{\mathcal{S}})/T}$ and $Z = \sum_{C_{\mathcal{S}}} e^{-E_{\mathcal{S}}(C_{\mathcal{S}})/T}$, the Shannon entropy $\mathbf{S_{can}}$ is

$$\mathbf{S_{can}} = \ln Z + \beta < E(C_{\mathcal{S}}) > .$$

3.3 Maximum Likelihood States and Phase Transitions

Phase transitions are sudden onset of a macroscopic phenomenon when a system parameter crosses a critical value. We are familiar with reversible phase transitions such as water to ice and ice to water. (In more complex dynamics, catastrophic (irreversible) system bifurcations may occur at critical parameter levels.) We will now see how magnetization occurs below a critical temperature in an Ising model with fully connected geometry.

Fully Connected Ising Model

Consider the Hamiltonian

$$E_R = -\frac{J}{N} \sum_{i<j} s_i s_j + E_0.$$

Note that the spins in the summation are 'fully connected' rather than 'nearest-neighbors'. The factor of N is therefore needed in the denominator to keep the energy per spin from diverging to infinity as $N \to \infty$. In this setting:

- The energy can be expressed in terms of the magnetization $M = \sum_{i=1}^N s_i$ as (**Exercise 3.3.1**)

$$E_R = -\frac{J}{2} N m^2,$$

where $m = M/N$ is the magnetization per spin and $E_0 = -J/2$.

- The distribution of the magnetization per spin m is given by [Bertin 2021]

$$P(m) = \frac{1}{Z} \sum_{C:m(C)=m} e^{-\beta E(C)} = \frac{1}{Z} e^{\mathbf{S}(m)+\frac{1}{2}\beta N m^2}$$

  where the number of configurations with magnetization m is

$$\Omega(m) = e^{\mathbf{S}(\mathbf{m})} = \frac{N!}{N_+!N_-!}$$

  and

$$N_+ = \frac{N}{2}(1+m) \text{ and } N_- = \frac{N}{2}(1-m).$$

One can show that [Bertin, 2021]

$$P(m) = e^{-Nf(m)}$$

where

$$f(m) = f_0(T) + \frac{1}{2}(1 - \frac{J}{T})m^2 + \frac{1}{12}m^4 + O(m^6)$$

and $f_0(T)$ is a temperature dependent constant to ensure $f(m) \geq 0$.

The following phase transition occurs (**Exercise 3.3.2**):

- If $T \geq T_{crit}$, $f(m)$ has a single minimum point that occurs when $m = 0$. (no magnetization occurs)
- If $T < T_{crit}$, $f(m)$ has two symmetric minimum at $\pm m_0$. (positive/negative magnetization occurs)

Exercises

3.3.1 Show that for the fully connected Ising model,

$$E_R = -\frac{J}{2} N m^2,$$

where $m = M/N$ is the magnetization per spin.

3.3.2 Consider the function $f_T(m) = \frac{1}{2}(1 - \frac{1}{T})m^2 + \frac{1}{12}m^4$. Show that there exists a critical value T_{crit} such that $f_T(x)$ has a single absolute min at m=0 when $T \geq T_{crit}$ and symmetric absolute min at $m = \pm m_0$ when $T < T_{crit}$.

3.4 Simplified Schelling Model and Segregation

The Schelling model is an example of how the ideas of statistical physics might be applied within urban science. The Schelling model represents dynamics of residential moves within a city. The city is modelled as a checkerboard divided into cells. Two types of agents reside in the city, with at most one agent in each cell. A utility function u describes the degree of satisfaction of each agent with the neighborhood in which they reside and governs the dynamics of agent moves. Segregation consists of areas with higher densities of one type of agent.

A simplified Schelling model [Bertin 2021] considers only one type of agent and considers segregation in the form of areas which have higher densities of agents (as opposed to a homogeneous density throughout the city). In the simplified model,

- A city is divided into a large number Q of blocks.
- Each block contains H cells.
- A macroscopic configuration C of the city consists of a knowledge of the state (empty or occupied) of each cell.
- Each cell contains at most one agent, so the number of agents n_q in a given block q ($q = 1, 2, ..., Q$) satisfies $n_q \leq H$.
- The density of agents is $\rho_q = n_q/H$.
- Each agent has the same utility function $u(\rho_q)$ which indicates the degree of satisfaction with the block the agent lives in.

The discrete-time movement of the agents in the city follow these rules [Bertin 2021]:

- Agents can only move from one block to a different block.
- At each time step, one agent and one empty cell in a different block are selected at random.
- The probability that the agent moves to the empty cell is

$$W(C' \mid C) = \frac{1}{1 + e^{-\Delta u/T}}$$

  where C and C' denote the respective configurations before and after the move.
- Δu is the change in utility in moving to the empty cell.
- The parameter T (analogous to temperature) takes into account factors such as presence of services, shops, friends etc. that influence the decision to move.
- The model is individualistic in that the probability of moving only depends on the agent's own change in utility. It does not consider the potential impact on other agents.
- The balance equation is

$$W(C' \mid C)P(C) = W(C \mid C')P(C')$$

  with

$$P(C) = \frac{1}{Z}e^{-F(C)/T}$$

where Z is the analog to the partition function and

$$F(C) = -\sum_{q}\sum_{m=0}^{n_q} u(\frac{m}{H}).$$

To study segregation, in equilibrium, the probability distribution of the block densities (with the sum of the densities held constant) has the form [Bertin 2021]

$$P(\rho_1, ..., \rho_Q) = Kexp(-\frac{H}{T}\sum_{q=1}^{Q} f(\rho_q))$$

with $H, T > 0$.

A homogeneous (non-segregated) density ρ_0 is unstable if there exist two densities ρ_1 and ρ_2 such that [Bertin 2021]

$$\gamma f(\rho_1) + (1-\gamma)f(\rho_2) < f(\rho_0).$$

The parameter γ $(0 < \gamma < 1)$ corresponds to the fraction of blocks that would have a density ρ_1 in the segregated state. This condition means that the value of the potential Φ is lower for the segregated state than the homogeneous state (see **Exercise 3.4.1**). Such densities can be located geometrically as points of 'bitangency' [Bertin 2021] (see **Figure 16** and **Exercise 3.4.2**).

Exercises

3.4.1 Show that in equilibrium the maximum likelihood configurations of densities $(\rho_1, ..., \rho_Q)$ minimizes the potential function ('free energy') $\Phi(\rho_1, ..., \rho_Q)$ defined as

$$\Phi(\rho_1, ..., \rho_Q) = \sum_{q=1}^{Q} f(\rho_q). \tag{7}$$

3.4.2 Find a line which is a tangent to the quartic $y = f(x) = x^4 - 2x^2 - x + 1$ at two different points $P = (p, f(p))$ and $Q = (q, f(q))$, Sketch the quartic and bi-tangent line.

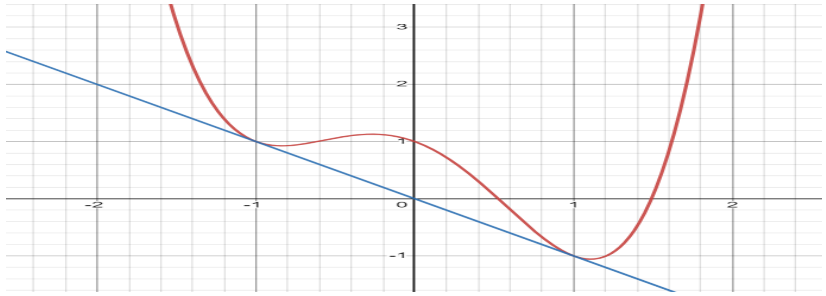

Figure 16. Example of a bitangent.

4. Societal Applications

Perhaps the most obvious example of complex social systems and justification for urban science is the proliferation of large metropolitan cities.

- RAPID URBANIZATION: The vast majority of those living a traditional subsistence existence are projected to move to urban environments. In 2007, the world's urban population surpassed the rural, and in 2021, the latter peaked and is now in decline [Bettencourt 2021]. The emergence of major metropolitan areas has shifted inter-connectivity of people from familiar local relations to global business between strangers.
- TRANSFORMATIVE POWER: Urban environments have enormous transformative power which compels a scientific understanding of how cities grow and impact their environment. There is a positive correlation between urbanization and economic and human development [Bettencourt 2021]. Informed/uninformed political decisions influencing large, high-density masses of people may build or destroy civilization.

In this section, we give three examples of urban data analysis which draw on concepts introduced earlier in this Module. A fourth example returns to consideration of a complex problem in post-war Tigray, Ethiopia; namely, the plight of internally displaced people (IDP).

4.1 Incarceration and Parole

The U.S. correctional system is large and complex. Although every individual in the penal population is different, Raphael [2011] describes a dynamical system categorizing the U.S. population into one of three states: (a) Not Incarcerated, Not on Parole, (b) Incarcerated, (c) Parole. , **Table 1** gives the probability that an individual will transition from one state to another in 1980 and also in 2005. The macroscopic state (percentage in each category) while in flux, may be expected to approach a steady state in the absence of policy changes. Determining the steady state populations associated with these transition probabilities is one way to assess improvement or deterioration of the criminal justice system over this 25 year period.

To this end, in 1980, the probability that someone on Parole (third row) transitioned to Not Incarcerated, Not on Parole was roughly .40; the probability that someone on Parole transitioned to being Incarcerated was .13; and the probability that a person on Parole remained on Parole was .47. Notice that the sum .40+.13+.47 =1 since the three states are the only possible states to which a parolee can transition. Each of the rows in the transition matrices must add to 1 for the same reason.

Table 1. **Comparison of three-state transition probability matrix for 1980 and 2005. Data source: Rafael [2011]**

	Destination state		
Origin State	Not Incarcerated, not on parole	Incarcerated	Parole
	A : 1980		
Not Incarcerated, not on parole	0.99937	.00063	0
Incarcerated	0.08211	0.52830	0.38958
Parole	0.40390	0.13073	0.46538
	B : 2005		
Not incarcerated, not on parole	0.99826	0.00174	0
Incarcerated	0.12697	0.50629	0.36674
Parole	0.29738	0.29335	0.40927

Transition matrices can be used to compute the equilibrium levels for each of the 3 groups (Not Incarcerated-Not on Parole, Incarcerated, Parole). The steady states are the proportion of the total population comprised by each group.

We now describe mathematically how the steady state incarcerated is computed for 1980 using a simplified transition probability matrix based on section A of **Table 1**. Consider the transition matrix M defined as follows:

$$\begin{pmatrix} .999 & .08 & .4 \\ .001 & .53 & .13 \\ 0 & .39 & .47 \end{pmatrix}$$

Note that this is the transpose of the entries in **Table 1**.

Let the steady state population levels be x_1 (Not incarcerated, Not on parole), x_2 (Incarcerated), x_3 (Parole). Then x_1, x_2, x_3 as steady state values must by definition satisfy $x_1 + x_2 + x_3 = 1$ and also

$$\begin{pmatrix} .999 & .08 & .4 \\ .001 & .53 & .13 \\ 0 & .39 & .47 \end{pmatrix} \begin{pmatrix} x_1 \\ x_2 \\ x_3 \end{pmatrix} = \begin{pmatrix} x_1 \\ x_2 \\ x_3 \end{pmatrix}.$$

Thus the steady state is an eigenvector of the transition matrix M with eigenvalue 1:

$$\begin{pmatrix} x_1 \\ x_2 \\ x_3 \end{pmatrix} = \begin{pmatrix} .995 \\ .003 \\ .002 \end{pmatrix}$$

Since the steady states values are $x_1^* = .995$, $x_2^* = .003$, and $x_3^* = .002$ the Not Incarcerated, Not on Parole population steady state proportion is 99.5% of the total population. The steady state Incarcerated population is .3% and the Parole population is .2%. An equilibrium is stable if nearby states converge to the equilibrium state as time progresses. Otherwise, the equilibrium is unstable. In this case, the graph shown in **Figure 17** suggests these equilibrium values are stable.

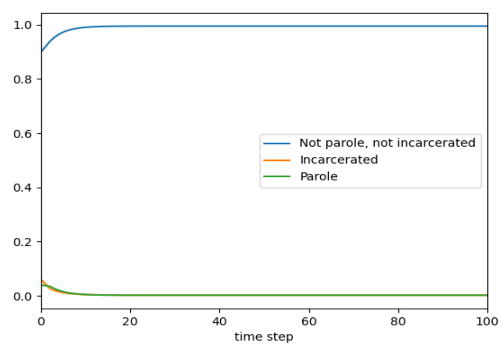

Figure 17. Graph with initial values $(x_1, x_2, x_3) = (.9, .06, .04)$ indicates stablity of the steady state levels $x_1^* = .995$, $x_2^* = .003$, and $x_3^* = .002$.

Exercise

4.1 Find the steady state values for 2005 and comment on its similarities/ differences with the steady state values for 1980.

4.2 Urban Productivity

A city's productivity is a basic socio-economic indicator often measured by GDP per capita. Such an indicator follows a power scaling law of the form

$$GDP_i = aN_i^s$$

where a and s are constants and N_i is the population of city i. Note that given GDP and population data for N cities, the scaling law implies that

$$\ln GDP_i = A + s \ln N_i.$$

with $A = \ln a$. In other words, the power s may be obtained by OLS regression of data points $(\ln N_i, \ln GDP_i)$ $(i = 1, ..., N)$ as shown in **Figure 18**.

SAMI (Scale Adjusted Metropolitan Index) uses the residuals (deviation from the expected power law scaling) rather than the (log of the) GDP values to assess city performance. One notes that Suzhou has an exceptionally large

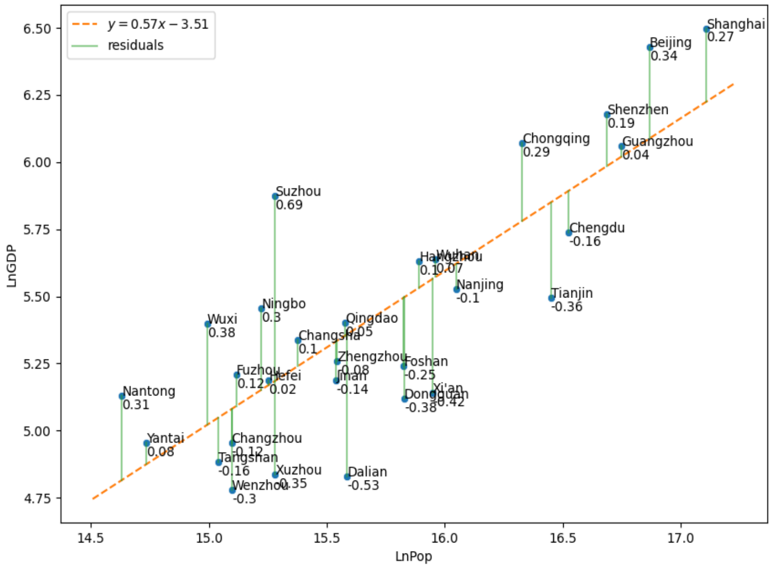

Figure 18. SAMI for GDP of the largest cities in China shows the scaling behavior as a regression line and uses residuals to assess city productivity.

residual. In fact, Suzhou experimented with a central business park patterned after Singapore and became one of the most highly developed and prosperous cities in China.

Exercise

4.2 Where would Hong Kong fall if added to the SAMI graph (**Figure 18**)?

4.3 Job Diversification

Another interesting and important question about cities is their degree of business diversification. According to US Bureau of Labor Statistics data (https://www.bls.gov/oes/tables.htm) Abilene, TX has over 70,000 jobs which can be classified into 290 types. Using data for a large number of cities, one can look for a scaling law of the form

$$D_S(N) = cN^s,$$

where $D_S(N)$ is the expected number of different job types for a city of size N. (Note that the value of $D_S(N)$ depends on the resolution of job classification.) Then as before, one can use SAMI to assess the amount of job diversification for a given city.

Business types have various classifications, including the North American Industry Classification System (NAICS), a hierarchical taxonomy with resolution levels 2-6. Level 2 consists of the broadest sectors such as '71 arts and entertainment' and level 6 is the most specific classification of business types, such as '711110 dinner theater'. The histogram in **Figure 19** is a histogram of the number of jobs in each job type.

Data for this histogram specifies empirical probabilities that a job is of a given type. Thus, the types can be ranked in terms of decreasing empirical probabilities $P(i)$. The Shannon entropy $H = -\sum_{i=1}^{D_S} P(i) \ln P(i)$ where $D_S = 290$ is thus a measure of job diversification in Abilene.

Exercise

4.3 Consider the following distributions of students turning in late assignments for three different classes:

a) For each of the three class distributions, compute the Shannon entropy

$$H = -\sum_{i=0}^{4} P(i) \ln P(i)$$

where $P(i)$ denotes the empirical probability that a student turns in i late assignments.

b) In this context, why does higher entropy indicate higher disorder?

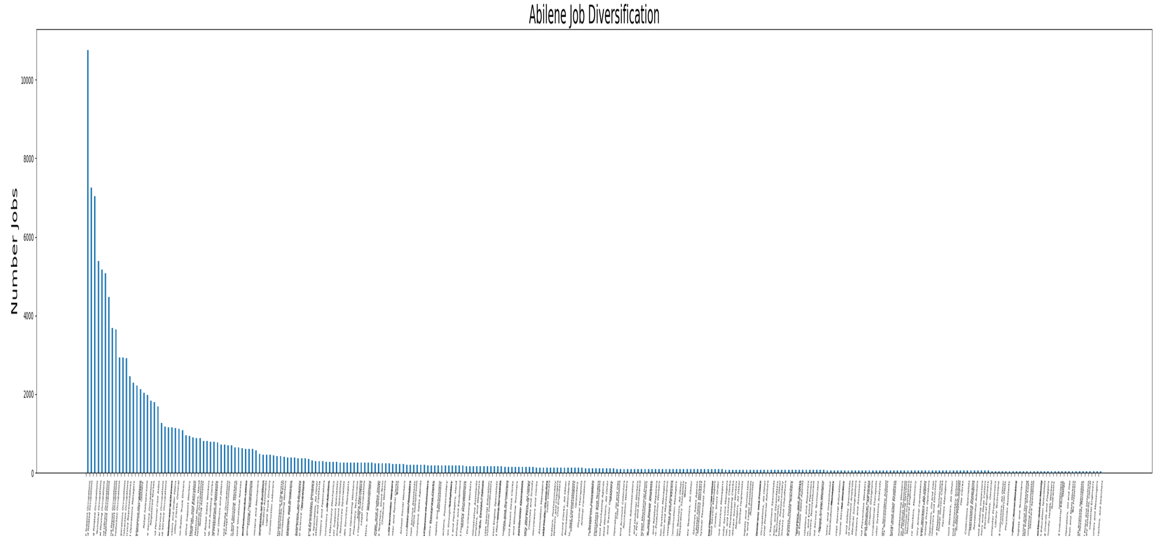

Figure 19. Abilene TX has over 70,000 jobs classified into 290 types. Data Source: US Bureau of Labor Statistics https://www.bls.gov/oes/tables.htm

Class	Number Students	Number Late Assignments			
		0	1	2	3
C1	30	30	0	0	0
C2	20	19	1	0	0
C3	25	15	5	2	3

4.4 A Simple IDP Response Model

Between Nov 2020 and Nov 2022, the Tigray region in northern Ethiopia suffered a horrific civil war. At one point their were an estimated 2.5 million internally displaced people (IDP) out of a population of 6-7 million. Even a year after the Pretoria Peace agreement, fighting by tribal militia continued in western Tigray, leaving 1 million IDPs. If the IDP problem were the only problem, the situation would be complex. The instability caused by the on-going fighting, widespread trauma due to a huge number of civilian deaths and rape victims, a crippled infra-structure in multiple sectors (eg. health, education) left leaders wondering where to begin the reconstruction.

IDP Data

We considered the data set 'DTM Ethiopia - SA - Tigray - R33XLSX (1.4M)' (downloaded on 12/18/23 from https://data.humdata.org/dataset/ethiopia-displacement-northern-region-tigray-idps-site-assessment-iom-dtm?). This data was published by the U.N.'s International Office of Migration (IOM), gives information about IDP camps collected in Summer 2023, and was last modified on August 11, 2023 (Round 33). The dataset contains 638 rows and 468 columns, and thus has information for more than 600 IDP camps. **Figure 20** summarizes the 468 columns of information provided.

.

Simplifying Assumptions on IDP System Complexity

The complexity of the IDP situation is reduced by two simplifying assumptions:

- Data Reliability: the IOM data set for over 600 IDP camps is regarded as accurate. For example, number of IDPs in a camp, age and gender breakdown, and classification of a camp's overcrowding are not questioned.
- Static Equilibrium: We also assume that the 600+ IDP camps scattered across most of Tigray are stable (neither movement of IDP from one camp to another, nor formation of new camps or closing of existing camps.)

A model's output would therefore only have a certain temporal validity and would need to be re-run on future updates to the IOM data.

A Basic Response Model

Category	Subcategory
Communication	News sources: QF-QU Mobile network/phones: QU-QV Travel: QW-QZ
Demographics	BJ-CE
Displacement	Initial Cause: CF-DD Prevented Return: DE-EF
Education	Boy attendance barriers: OI-PC Girl attendance barriers: NM-OH Pre-primary: MF-MJ Primary: MK-MO Quality/satisfaction: MZ-NL Resources: MV-MY Secondary: MP-MT Teachers: MY, NG, NH
Food	Distribution Sites: IL-IZ Fuel: GB-GC Markets: GD-GE, JA-JL, MW School Programs: MX, NP, OL
Hygiene	Hand-washing: IC-IK Women's needs: NW
Healthcare	Location and services: LP-MA Malnutrition Treatment: JQ-JR Mobile Healthcare Teams: JZ-KA Mosquito net: AV, FS, ME MUAC Screening: JM-JP Problems in health: KC-KH Problems in healthcare access: KI-LO School Programs: MX, NP, OL TSFP (Targeted Supplementary Feeding): JS-JY, KB Women's needs: JM, JU, MB-MD, NW
Latrines	Number/Quality: HG-HM, MU Problems: HN-IB Schools: MU, OD, OY
Livelihood	Access to income: PD-PF Farming: QD-QE Livestock: PG-PT, QB-QC Loss of resources: PU Programs: PV-PZ
Shelters	Basic Information: EG-EQ Materials: ER-GA
Site	2 Largest IDP needs: AS-BI 2 Largest IDPs: AK-BI Basic Information: A-X Support Management: Y-AJ
Water	Cooking, Hygiene: GO Distribution: GH-GI Drinking Water: GL-GN, MJ, MO, MT, OE, OZ Hygiene: IC-IJ Problems: GP-HF Treatment: GJ-GK Water Sources: GF-GG

Figure 20. IOM IDP data with Excel sheet column references.

With such overwhelming needs and very few NGOs responding due to the continued instability and travel warnings, we first considered the following practical assignment problem: to which IDP camp should a given NGO respond? We used the following two criteria as the basis for assignments:

- Effectiveness: The first criteria we considered is effectiveness of a response. That is, an NGO should only be assigned to an IDP camp for which it has sufficient resources to meet the need.
- Child Vulnerability: The second criteria we considered is child protection: what proportion of the camp population is children under the age of 3?

We first designate the need categories under consideration $1, 2, ..., k$. For example 1 might be food, 2 shelter, etc. Each camp has a state vector

$$s = < s_1, s_2, ..., s_k >$$

where $s_i = 1$ if the camp has need i and 0 otherwise. For simplicity we assume the need of the camp is given by

$$Ns = < Ns_1, Ns_2, ..., Ns_k >$$

where N is the number of people in the camp.

Each NGO has a capacity vector of the form

$$< n_1, n_2, ..., n_k >$$

where n_i indicates the number of people for which it can supply need i. An IDP camp with need Ns is feasible for an NGO if and only if

$$Ns = < Ns_1, Ns_2, ..., Ns_k > \preceq < n_1, n_2, ..., n_k >,$$

where $p \preceq q$ if each component of p is less than or equal to the corresponding component of q. **Figure 21** shows a basic response model output which maps effective response options for a hypothetical NGO. Clicking on an icon gives the camp name and proportion of children under 3. (See the JNB "IDP Response" available at https://drive.google.com/drive/folders/1zqQB-hEPocxOVOjiI0Q32XDKVJoq6PI3?usp=sharing.)

Complexity of a Response Region

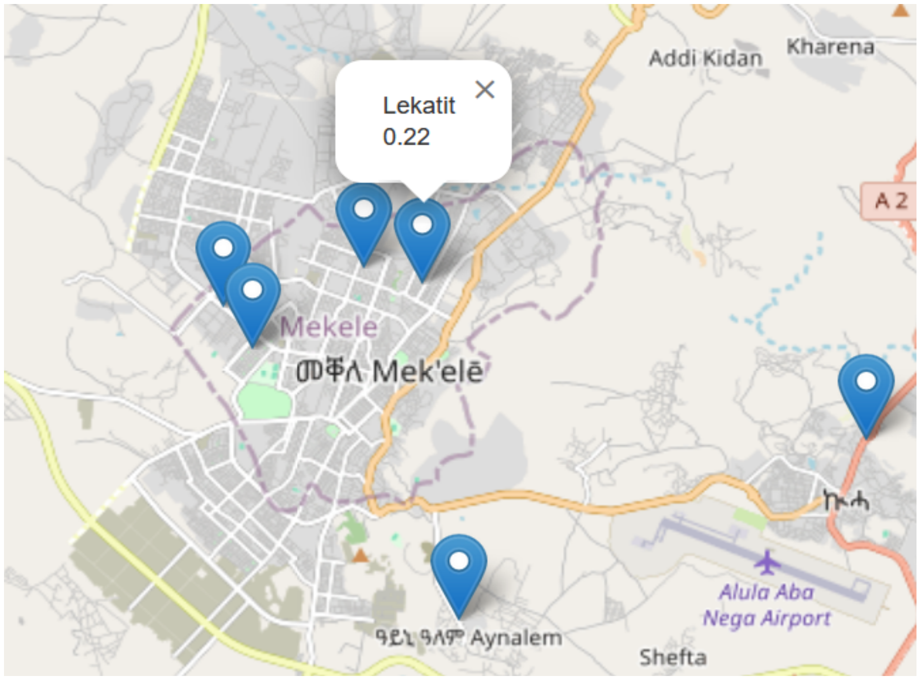

Figure 21. Hypothetical NGO's map of effective response IDP camp locations with proportion of children under age 3. See the JNB 'IDP Response' available at https://drive.google.com/drive/folders/1zqQB-hEPocxOVOjiI0Q32XDKVJoq6PI3?usp=sharing

Note that we can use entropy to measure the amount of disorder in a given area with N IDP camps. Let p_i be the empirical probability that a camp has need $i \in \{1, 2, ..., k\}$. Then the entropy H is computed as

$$H = -\sum_{i=1}^{N} p_i \ln p_i.$$

.

For example,

- if all the camps have need $i = 1$ (eg. food) and no other need, then $p_1 = 1$, all other $p_i = 0$, and hence $H = 0$.
- if all camps have all the needs $1, ..., k$, then $p_i = 1$ for all i, and again $H = 0$.
- if the probability that a camp has need i is $1/i$, then $H_N = \sum_{i=1}^{N} \frac{\ln i}{i}$. Note that in this case, the needs are ordered by frequency of occurrence. A graph of H_N is shown in **Figure 22**

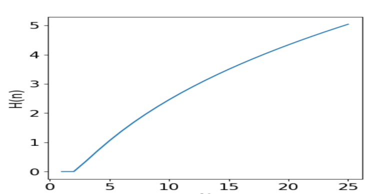

Figure 22. Graph of H_N for the case where the probability of need is $p_i = 1/i$ ($i = 1, ..., N$)

.

Entropy can be used to measure disorder for the entire Tigray region. If all camps have exactly the same needs (coherent system with $H = 0$), the response to the needs is conceptually less complex than the case when there are varying needs (correlated system, $H > 0$). Note that if peace is restored in such a way that all camps are vacated and the IDP return to their homes, this is a special case where all camps have the same need: $p_i = 0$ for all $i \in \{1, ..., k\}$. Civil war resulted in a tragic phase transition from $H = 0$ to $H > 0$.

Exercises

4.4.1

Suppose a group of x NGO's denoted $NGO_1, ..., NGO_x$ are considering a response in a region R with y camps denoted $Camp_1, ..., Camp_y$ (we assume $x \leq y$). An effective total response is of the form

$$< a_1, a_2, ..., a_x >$$

where $Camp_{a_i}$ is feasible for NGO_i ($i = 1, 2, ..., x$). What is the probability of a random assignment being effective if there are f effective total responses?

4.4.2 Suppose NGO_i has a utility function which measures its preference for a feasible assignment to a camp a_i. Utility is measured by efficiency. For example, a camp which is easier to reach (lower total cost to transport staff and materials) would have higher utility. Explain how effective total responses might be rank-ordered by efficiency.

4.4.3 How might a basic response model be modified in the case where there are no effective total responses (overwhelming needs) ?

4.5 Mini-Modeling Problem

Returning to the problem posed at the beginning of this Module, suppose an NGO provides educational support for IDPs and is considering working in either Mekelle or Shire (the two largest cities in Tigray with the most IDP). Using the data IDP.xlsx available at https://drive.google.com/drive/folders/1zqQB-hEPocxOVOjiI0Q32XDKVJoq6PI3?usp=sharing, develop a model which can be used to determine which between Mekelle and Shire has the greater disorder in its IDP camp education sector.

5. Discussion

In this Module, we have introduced a few intuitive ideas about complex systems (**Section 2**), examined some of the underlying mathematical concepts such as equilibrium, phase transition, and entropy from statistical physics (**Section 3**), and provided examples how these concepts might be applied to empirical data about complexity in human society (**Section 4**). We refer the reader to Fieguth [2021] (**Section 2**), Bertin [2021] (**Section 3**) and Bettencourt [2022] (**Section 4**) for in-depth treatments of this material. The applicability of calculus, differential equations, and probability reinforces the value of undergraduate level mathematics.

We also hope to have raised awareness of the plight of IDP in the Tigray region of Ethiopia. While writing this Module, the authorship team was involved in a 'Math Serve', communicating with the Mayor of Nebelet who was overseeing an IDP camp of 266 people living in a school (IDP center). Since our team leader visited Nebelet in August 2023, we knew that a primary need was emergency food supply. Problems we encountered setting up food delivery included the right quantity and timing of deliveries (roughly 10 quintiles per month), as well how to ensure the quality of the food being delivered. Even so, the IDP were very grateful for the food support.

A second need we considered was IDP housing. As classrooms are in great demand, the IDP need to be relocated. One affordable housing option is a $ 125 tent large enough for one household (**Figure 23**). Though affordable, unless

Figure 23. Tents used for IDP households.

the IDP are living at a registered center, they will not be eligible to receive a number of benefits including food aid, non-food items, cash support, re-settlement packages etc. We searched the IOM IDP camp data for registered IDP camps close to Nebelet with low overcrowding and within the Mayor's woreda jurisdiction. Only 1 camp met these criteria, namely Adihedem which has 960 IDP and is 16 km from Nebelet. Adihedem, however, has food and water shortages, and over 75% of the IDP are staying with families. The Mayor recommended building a new IDP center with 68 tents (one for each household) 1 km from the school in Nebelet. The Math Serve team discussed ideas for an "IDP Tent Village" (**Figure 24)**. In developing a design in consultation with the Mayor and NGOs potentially involved in constructing such a tent village, we learned that there would be both water and electric supply available on site, and that the area did not need a security fence since it would be police-patrolled at night. At the time of writing of this Module we were waiting for answers to several important questions from our partners on the ground: (i) would all the IDP be happy to move to such a tent village? (ii) Would vegetable gardens next to the tents cause any problems such as bugs/rodents? (iii) how durable are the tents and are they available in sufficient quantity in Mekelle? (iv) Could such a village be registered by the IDP governing bodies?

Figure 24. Preliminary idea for the layout of an IDP tent village.

As a big scale 'reality check', the U.N. spent millions of dollars to build a large IDP camp about 7 km southwest of Shire. But none of the tens of thousands of IDP living in Shire (see **Figure 25**) wanted to move there since it was not within easy walking distance to the city where the IDP beg for food. Furthermore, firewood was not available for cooking, and to compound matters, it was close to an army base, raising safety concerns. Plans which are not well-connected to the community/beneficiaries' needs and preference may look good on paper but in fact be unrealistic and result in a huge waste of time and material resources if implemented.

Figure 25. IDP camp populations in Shire.

From complex system theory we know that in some cases a transition can be catastrophic or irreversible. Our prayers are with the people of Tigray that the effects of the horrific civil war will be reversible in the sense that a stable and peaceful society will soon be restored. Our hope is that readers of this Module will be moved to participate in some way in an open system for the restoration of Tigray to the beautiful land that it once was.

6. Solutions to Exercises

2.1 A puzzle with only 1 or 2 types of pieces will be less complex than a jigsaw puzzle where each piece is unique. For complex problems in human society, a major challenge is how to limit the characteristics of constituent parts so the entire population is subdivided into major types whose analysis gives a good picture of the state of the system as a whole. (Such a strategy is also used within statistical physics in the form of the re-normalization group approach [Bertin 2021].)

2.2.1 Rebuilding may be impossible within an isolated rural community. In a major metropolitan area such as Mekelle, the regional capital, distance learning facilitated by international money transfer can turn an isolated learning system into a closed system (transfer of 'energy' in the form of credit and knowledge but not physical resources). The post-war rural Embasneyti school district became an open system in August 2023 when it received a 'mass transfer' of 80 blackboards, 6000 notebooks, pens and pencils, 3 laptops and 16 soccer balls. This enabled the relaunch of school for 6,000 children in the district, and was a story covered by regional TV media (https://www.facebook.com/yohans.teklemariam/videos/1018050329637169/?d=w&mibextid=2PtUEq)

2.2.2 If each IDP camp had the same characteristics (size, types of needs, registration with the government etc.) response to the IDP crisis would be much simplified due to coherence. In the absence of such coherence, a survey of IDP camps may be administered on an ongoing basis based on criteria such as shown in **Figure 20**. The response data could then be used to measure similarity (correlation) between camps as well as track changes to each camp over time.

2.2.3 When a sheet of graph paper is filled using Wolfram's Rule 90, the result is shown in **Figure 26**. Note the emergence of a fractal structure (Sierpinski triangle).

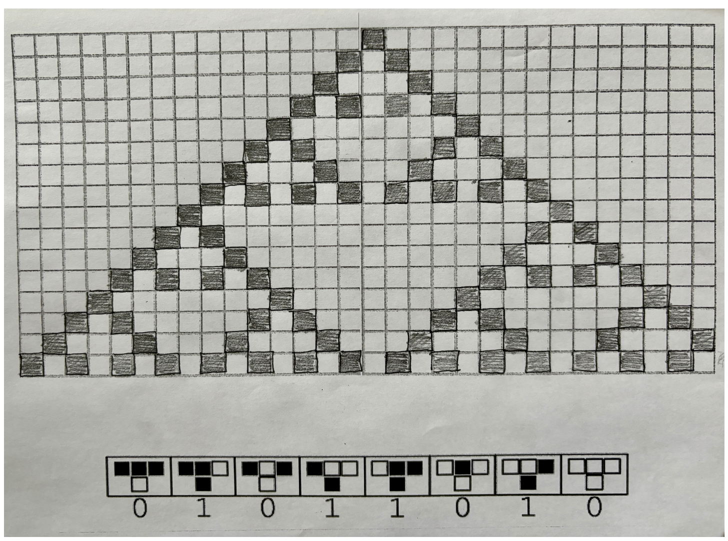

Figure 26. Solution to **Exercise 2.2.3**

2.3.1 Let λ_1, λ_2 be the two eigenvalues of the Jacobian matrix, A. The qualitative behavior of the nonlinear system near P depends on the signs of the eigenvalues. When both eigenvalues are real: If $\lambda_1 > \lambda_2 > 0$, the system will be an unstable node, shown in the far right of quadrant I in **Figure 7**. If $\lambda_1 < \lambda_2 < 0$, the system will be a stable node, as shown in the far left of quadrant II in **Figure 7**. When $\lambda_2 < 0 < \lambda_1$, the system will behave as a saddle point, as is shown in **Figure 7** in quadrants III and IV.

The cases when there are complex eigenvalues are shown in **Figure 7** in the region above the parabola $4detJ = tr(J)^2$. In this case, the eigenvalues are $\lambda_{1,2} = \alpha \pm i\beta$. Then, when $\alpha < 0$, the system will be a stable spiral. When $\alpha > 0$, the system will be an unstable spiral. Finally, when $\alpha = 0$, the system will be a centre, shown along the y-axis of **Figure 7**.

2.3.2 Let J denote the Jacobian matrix $\begin{pmatrix} \frac{\partial f}{\partial x} & \frac{\partial f}{\partial y} \\ \frac{\partial g}{\partial x} & \frac{\partial g}{\partial y} \end{pmatrix}$. In our case, $\frac{dx}{dt} = 3x - y^2 = f(x,y)$ and $\frac{dy}{dt} = sin(y) - x = g(x,y)$,

so we have $J = \begin{pmatrix} 3 & -2y \\ -1 & cos(y) \end{pmatrix}$. At $(0,0)$, $J = \begin{pmatrix} 3 & 0 \\ -1 & 1 \end{pmatrix}$.
The eigenvalues of $J(0,0)$ are $\lambda = 1, 3$. Therefore, this system is a source, and the equilibrium (0,0) is unstable.

2.4.1 See the JNB "Complex Systems Lab" available at https://drive.google.com/drive/folders/1zqQB-hEPocxOVOjiI0Q32XDKVJoq6PI3?usp=sharing.

2.4.2 As can be shown in **Exercise 2.4.1**, when $K > 0$ is small, a stable steady state occurs at $(0, C_*)$ with $C_* > 0$ For higher values of K, the equilibrium point $(0, C_*)$ loses its stability and there is a new stable steady state (F^*, C^*) with $F^* > 0, C^* > 0$. For even higher values of K, the equilibrium (F^*, C^*) is a spiral sink. For still higher values of K, the spiral equilibrium (F^*, C^*) loses its stability and a stable limit cycle (closed curve) solution appears. The bifurcation diagram follows this pattern, showing a stable equilibrium $(F_* = 0, C_* > 0)$ for $K < k_1$. This equilibrium loses its stability at $K = k_1$ and there arises a new stable equilibrium (F^*, C^*) with $F^* > 0$ and $C^* > 0$. At $K = k_2$, a Hopf birfucation occurs: the stable equilibrium point (F^*, C^*) loses its stability and a stable limit cycle appears for $K > k_2$.

2.4.3

a) To find a period one point for $x_{n+1} = rx_n(1 - x_n)$, we substitute x_n for x_{n+1} and solve for x_n.

$$x_n = rx_n(1 - x_n)$$

$$0 = -rx_n + rx_n^2 + x_n$$

$$0 = x_n(1 - r) + rx_n^2$$

$$0 = x_n(1 - r + rx_n)$$

So, $x_n = 0$, $x_n = \frac{r-1}{r}$ are the two fixed points we find. Therefore, when $1 < r < 2$, $\frac{r-1}{r}$ is a period one point for this map.

b) The Feigenbaum constant $\delta = \lim_{n\to\infty} \frac{r_{n-1} - r_{n-2}}{r_n - r_{n-1}} = 4.669\,201\,609\ldots$ is a universal constant for period doubling bifurcations in 1D maps.

2.5 See the JNB "Complex Systems Lab" available at https://drive.google.com/drive/folders/1zqQB-hEPocxOVOjiI0Q32XDKVJoq6PI3?usp=sharing.

3.1.1 We know that $\frac{dx}{dt} = v$ and $v = \frac{p}{m}$. So, $\frac{dx}{dt} = \frac{\partial H}{\partial p}$ since the partial derivative of H with respect to p is $\frac{p}{m}$.
We also know that $\frac{dp}{dt} = F$ and $F = -kx$. So, $\frac{dp}{dt} = \frac{-\partial H}{\partial x}$ since the partial derivative of H with respect to x is kx.

3.1.2 $\frac{dE}{dt} = (\frac{\partial H}{\partial x}\frac{dx}{dt}) + (\frac{\partial H}{\partial p}\frac{dp}{dt}) = (\frac{-dp}{dt}\frac{dx}{dt}) + (\frac{dx}{dt}\frac{dp}{dt}) = 0$.

3.1.3 Let $H = H(x^*, p^*) = \frac{(p^*)^2}{2m} + \frac{1}{2}k(x^*)^2$.

- $\frac{dx^*}{dt^*} = -\frac{dx(t^*)}{dt} = v^* = \frac{p^*}{m} = \frac{dH}{dp^*}$.
- $\frac{dp^*}{dt^*} = -m\frac{dv(t^*)}{dt^*} = m\frac{dv(t^*)}{dt} = ma(t^*) = -kx(t^*) = -kx^* = -\frac{\partial H}{\partial x^*}$.

3.2.1 First, observe that

$$E = -h\sum_{i=1}^{N} s_i = -hM, \qquad (s_i = \pm 1,)$$

Then, notice that:

$$M = N_+ - N_-$$
$$= N_+ - (N - N_+)$$
$$= 2N_+ - N$$

Similarly,

$$M = -2N_- + N$$

Next, we substitute in the values we just solved for M. We will first look at N_+

$$E = -h(2N_+ - N)$$
$$E = -2hN_+ + hN$$
$$2hN_+ = hN - E$$
$$N_+ = \frac{1}{2}\left(N - \frac{E}{h}\right)$$

Similarly for N_-, we substitute in the value we just solved for M. This leads to

$$E = -h(-2N_- + N)$$

and by algebra:

$$N_- = \frac{1}{2}\left(\frac{E}{h} + N\right)$$

3.2.2 First, we know that

$$ln(N!) \approx Nln(N) - N.$$

So,

$$\mathbf{S}(E) = ln\Omega(E) = ln(\frac{N!}{N_+!N_-!})$$
$$= ln(N!) - ln(N_+!) - ln(N_-!)$$
$$\approx NlnN - N - (N_+lnN_+ - N_+) - (N_-lnN_- - N)$$
$$= (-N + N_+ + N_-) + NlnN - N_+lnN_+ - N_-lnN_-$$
$$= ln\frac{N^N}{N_-^{N_-}N_+^{N_+}}$$

So, $\mathbf{S}(E) \approx ln\frac{N^N}{N_-^{N_-}N_+^{N_+}}$, as desired.

3.2.3

$$\Omega_{tot}(E_S|E_{tot}) = \Omega_S(E_S)\Omega_S(E_{tot} - E_S)$$

By maximum-liklihood,

$$\frac{\partial}{\partial E_S}\ln\Omega_S(E_S) + \frac{\partial}{\partial E_S}\ln\Omega_S(E_{tot} - E_S) = 0$$
$$\Rightarrow \frac{\partial}{\partial E_S}\ln\Omega_S(E_S) + \frac{\partial}{\partial E_R}\ln\Omega_S(E_R)\frac{\partial E_R}{\partial E_S} = 0$$
$$\Rightarrow \frac{\partial}{\partial E_S}\ln\Omega_S(E_S) - \frac{\partial}{\partial E_S}\ln\Omega_R(E_R) = 0$$
$$\frac{\partial}{\partial E_S}\ln\Omega_S(E_S) = \frac{\partial}{\partial E_S}\ln\Omega_R(E_R)$$
$$\frac{\partial\ln\Omega_S}{\partial E_S} = \frac{\partial\ln\Omega_R}{\partial E_R}$$

3.2.4 The formula for the grand-canonical distribution is merely a specific term divided by all the terms in the distribution. First, we must assume the system exchanges both energy and particles with the environment. Intuitively, this formula is finding the probability by dividing the particular configuration by the grand-canonical partition function, which is the sum of all possible configurations. So, this gives the probability that the particular configuration (C_S) occurs.

3.2.5

a)

$$
\begin{aligned}
-\sum_C P(C)\ln P(C) &= -\sum_C \frac{1}{\Omega(E)}\ln\frac{1}{\Omega(E)} \\
&= -\frac{1}{\Omega(E)}\sum_C \ln(\frac{1}{\Omega(E)}) \\
&= -\frac{1}{\Omega(E)}\Omega(E)\ln\left(\frac{1}{\Omega(E)}\right) \\
&\ln\Omega(E) = \mathbf{S}.
\end{aligned}
$$

b)

$$
\begin{aligned}
\mathbf{S} &= -\sum_C \frac{1}{Z}e^{-E(C_\mathcal{S})/T}\ln\left(\frac{1}{Z}e^{-E(C_\mathcal{S})/T}\right) \\
&= -\sum_C \frac{1}{Z}e^{-E(C_\mathcal{S})/T}\left(\ln\left(\frac{1}{Z}\right) - E(C_\mathcal{S})\beta\right) \\
&= [\frac{\ln Z}{Z}\sum_C e^{-E(C_\mathcal{S})/T}] + < E(C_\mathcal{S}) > \beta \\
&= \ln Z + \beta < E(C_\mathcal{S}) >
\end{aligned}
$$

3.3.1 Let $m = \frac{1}{N}\sum_{i=1}^N s_i$. Then

$$
-\frac{J}{2}Nm^2 = -\frac{J}{2N}(\sum_{i=1}^N s_i)^2 = -\frac{J}{2N}(2\sum_{i<j}s_is_j + \sum_{i=1}^N s_i^2) = -\frac{J}{N}\sum_{i<j}s_is_j - \frac{J}{2N}N = -\frac{J}{N}\sum_{i<j}s_is_j + E_0 = E_R
$$

where $E_0 = -\frac{J}{2}$.

3.3.2 Taking the derivative of the function $f_T(m)$ and setting it equal to zero, we obtain

$$
f_T'(m) = (1-\frac{1}{T})m + \frac{1}{3}m^3 = m[1-\frac{1}{T}+\frac{1}{3}m^2] = 0.
$$

The roots are

$$
m = 0
$$

and

$$
m = \pm\sqrt{\frac{3-3T}{T}}.
$$

If $T \geq 1 = T_{crit}$, then $m = 0$ is the only real root and is a minimun since $f_T''(m) = 1 - \frac{1}{T} + m^2$ is positive when $m = 0$ and $T > 1$.

If $T < 1$, then a minimum occurs at $\pm m_0$ where $m_0 = \sqrt{\frac{3}{T} - 3}$. (Note that $f_T''(m_0) = \frac{2}{T} - 2 > 0$.)

4.1 Similarly to the steady state for 1980, for the steady state for 2005, x_1, x_2, x_3 as steady state values must by definition satisfy $x_1 + x_2 + x_3 = 1$ and also

$$
\begin{pmatrix} .998 & .127 & .297 \\ .002 & .506 & .293 \\ 0 & .367 & .409 \end{pmatrix}\begin{pmatrix} x_1 \\ x_2 \\ x_3 \end{pmatrix} = \begin{pmatrix} x_1 \\ x_2 \\ x_3 \end{pmatrix}
$$

Once again, the steady state is an eigenvector of the transition matrix M with eigenvalue 1:

$$
\begin{pmatrix} x_1 \\ x_2 \\ x_3 \end{pmatrix} = \begin{pmatrix} .9897 \\ .0063 \\ .0039 \end{pmatrix}
$$

Thus, the steady state for the Not Incarcerated, Not on Parole population decreased slightly while the steady states for the Incarcerated population and Parole population both increased slightly from 1980 to 2005.

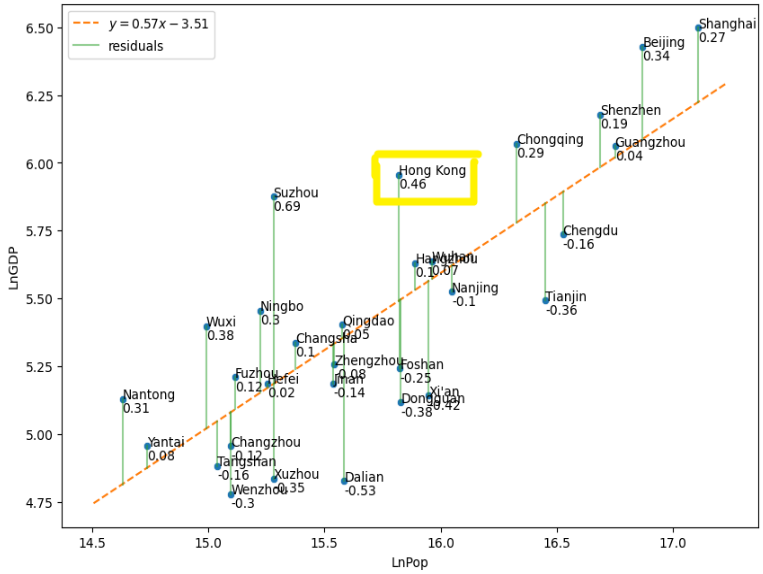

Figure 27. Solution to **Exercise 4.2**

4.2 If Hong Kong is added into the SAMI graph like **Figure 18**, the updated SAMI graph should look like the one below, where Hong Kong is highlighted:

See the JNB "Complex Systems Lab" available at https://drive.google.com/drive/folders/1zqQB-hEPocxOVOjiI0Q32XDKVJoq6PI3?usp=sharing.

4.3

a)

Class	Distribution of Late Assignments 0	1	2	3	Entropy H
C1	1	0	0	0	0
C2	.95	.05	0	0	.20
C3	.6	.2	.09	.12	1.1

b) Class C1 (all students turned in all assignments on time) is the most orderly and has entropy $H = -1\ln(1) = 0$. Class C2 was very orderly (only 1 out of 20 students had 1 late assignment) and a low entropy value ($H = -[.95\ln(.95)+.05\ln(.05)] = .20$). Class C3 had the highest entropy ($H = -[.6\ln .6+.2\ln .2+.09\ln .09+.12\ln .12] = 1.1$) with a considerable proportion of students students having 1,2, or 3 late assignments. This type of disorder can add a burden to the grading process and is one reason why teachers penalize or do not accept late assignments.

4.4.1 Note that there are $C(y,x) = \frac{y!}{x!(y-x)!}$ possible NGO assignments. Suppose f of these assignments are effective total responses. The probability of a random assignment being effective is $p = f/C(y,x)$.

4.4.2 The utility of an effective total response is the mean of the IDP assignment utilities for that response. Ordering assignments based on maximizing mean utility would thus be an efficient rank-ordering.

4.4.3 In cases where there are no effective total responses, a "need gap" might be introduced to measure how close an NGO is to meeting the need of a given IDP camp. Assignments could be made by minimizing the need gap for each NGO beginning with the NGO with the smallest amount of resources and ending with the NGO with the greatest amount of resources. The total need gap would be a measure of the total response effectiveness. A criteria such as maximizing child protection might be used to settle ties in total response effectiveness.

4.5 See the JNB "IDP Camp Entropy" available at https://drive.google.com/drive/folders/1zqQB-hEPocxOVOjiI0Q32XDKVJoq6PI3?usp=sharing. This JNB analysis found the educational entropy for Shire to be 2.14 and Mekelle to be 2.92, indicating the regional capital has a higher educational disorder in its IDP camps.

References

Bertin, E. 2021. *Statistical Physics of Complex Systems: A Concise Introduction (3rd Edition)*. Cham, Switzerland: Springer Nature.

Bettencourt, L. 2022. Introduction to Urban Science: Evidence and Theory of Cities as Complex Systems. Cambridge, MA: The MIT Press.

Fieguth, P. 2021. *An Introduction to Complex Systems: Society, Ecology, and Nonlinear Dynamics (2nd Edition)*. Cham, Switzerland: Springer Nature.

Ghosh, A. 2017. Dynamic Systems for Everyone: Understanding how our world works. (2E) Cham, Switzerland: Springer.

Isihara P, Diedrichs DR, Kartawijaya T, Townsend E, and Tully K. 2017. Disaster Relief Modeling, The UMAP Journal, Vol. 38(4):399-430.

Macauley, T. 2017. RIoT Control Understanding and Managing Risks and the Internet of Things. Amsterdam: Elsevier.

Martin, B. and de Roos, A. 2023. Hopf bifurcation in a predator-prey model. https://staff.fnwi.uva.nl/a.m.deroos/projects/QuantitativeBiology/43-HopfPoint-Rosenzweig.html

Murray, J.D. 2002. Mathematical Biology: I. An Introduction (3E). New York: Springer.

Sampson, R. 2012. Great American City: Chicago and the Enduring Neighborhood Effect. Chicago: The University of Chicago Press.

Siegenfeld, A. and Bar-Yam, Y. 2020. An introduction to complex system science and its applications. https://www.hindawi.com/journals/complexity/2020/6105872/

Tranquillo, J. 2019. An Introduction to Complex Systems: Making Sense of a Changing World. Cham, Switzerland: Springer Nature.

Acknowledgements

The project team is grateful to the Editor for his encouragement to write this Module, and to Mayor Kidanemariam and Ms. Karin van den Bosch for their help understanding the IDP situation in Nebelet and in Shire.